Spectrochimica Acta, Vol. 41A, No. 1/2, pp. 43–52, 1985
Printed in Great Britain.

0584–8539/85 $3.00 + 0.00

The vibrational spectra and force constant calculations of ethynylcyclohexane

T. WOLDBAEK, C. J. NIELSEN and P. KLAEBOE
Department of Chemistry, University of Oslo, Oslo 3, Norway

(*Received* 9 *July* 1984)

Abstract—The i.r. spectra of ethynylcyclohexane as a liquid and as amorphous and crystalline solids at 90 K were recorded between 4000 and 50 cm^{-1}. High pressure i.r. spectra of the liquid (1–20 kbar) and crystalline sample were recorded. Raman spectra of the liquid, including semiquantitative polarization measurements, were obtained and the amorphous and crystalline solids studied at 90 K.

The compound exists as an equilibrium of equatorial and axial conformers in the liquid and in the amorphous crystals while the molecule takes the *e*-conformer in the low temperature and high pressure anisotropic crystals. Under pressure the equilibrium is shifted towards the *a*-conformer in the liquid. In ethynylcyclohexane thiourea clathrate the *e*/*a* ratio is approximately eight times smaller than in the liquid, but the clathrate decomposes with time at ca 330 K.

A normal coordinate analysis was carried out, using a valence force field transferred from the halogenated cyclohexanes. It was extended with parameters for the side chain and fitted to the assigned fundamentals of the *e* and *a* conformers in cyano-, isocyano-, ethynyl- and *trans*-1,4-dicyanocyclohexane. The fundamentals of ethynylcyclohexane were correlated with those of cyano- and isocyanocyclohexane.

INTRODUCTION

Ethynylcyclohexane ($C_6H_{11}C{\equiv}C{-}H$), hereafter abbreviated ECH, is isoelectronic with cyano- ($C_6H_{11}C{\equiv}N$) and isocyano-($C_6H_{11}N{\equiv}C$) cyclohexane. All these compounds have substituents which are "narrow" groups of cylindrical symmetry. Unlike the cyano and isocyano groups the ethynyl has a negligible bond moment and the van der Waals radius on the carbon attached to the cyclohexane ring is supposedly higher for ethynyl- than for cyanocyclohexane [1]. In line with this prediction ethynylcyclohexane should give larger 1,3-syn axial repulsions to the hydrogens in the 3 and 5 positions than cyano- and isocyanocyclohexane. Nuclear magnetic resonance measurements have given ΔG^0 values for the equatorial-axial conversion equal to 1.68 kJ/mol (193 K, CS_2 solution) [2] and 2.11 kJ/mol (182 K, $CFCl_3$ solution) [1] by ^1H and ^{13}C techniques, respectively. Thus, the conformational equilibrium of ECH at the coalescence temperature (ca 195 K) will be approximately the same as for chloro-, bromo- and iodocyclohexane (ca 80% *e*, 20% *a*). For cyano- and isocyanocyclohexane the corresponding ΔG^0 values [1] are 0.877 and 0.778 kJ/mol, respectively, and the conformational equilibria more equally distributed (ca 60% *e*, 40% *a*).

In a microwave study of ECH an HCC ≡ angle equal to 106.3° in the equatorial, reduced to 102.4° in the axial conformer were reported [3]. These results confirm the 1,3- and 1,5-syn axial repulsions between the ethynyl and the hydrogens.

No vibrational spectroscopic study of ECH has to our knowledge been presented and the conformations present in the solid state are not known. In the present paper we shall report our results for ECH and compare the results with those obtained for cyano- and isocyanocyclohexane [4] and with the halocyclohexanes [5, 6]. Moreover, the normal coordinate analysis on ECH and on cyano- [4], isocyano- [4] and on *trans*-1,4-dicyanocyclohexane [7] combined in the overlay procedure will be described here, while the actual calculated wave numbers were given in the earlier papers.

EXPERIMENTAL

The sample of ECH was supplied by ICN Pharmaceuticals, Inc. and purified by distillation. A gas chromatographic analysis showed the purity to be better than 99%.

The i.r. and Raman spectrometers, the cells, cryostats and high pressure technique were described in a previous paper [4].

RESULTS

The i.r. spectra of ECH as an annealed crystalline solid at 90 K are shown in Fig. 1 (1000–400 cm^{-1}) and Fig. 2 (1185–1000 cm^{-1}). A solution spectrum in benzene is given in Fig. 3 and the corresponding crystal spectrum at 90 K in Fig. 4, both covering the far i.r. region 450–60 cm^{-1}. The i.r. spectra of ECH in the diamond anvil cell recorded at negligible pressure, at ca 20 kbar and as an anisotropic crystal at ca 25 kbar are shown in Fig. 5. Finally, Raman spectra of the liquid and an annealed crystal deposited at 90 K are shown in Figs 6 and 7, respectively. The wave numbers of the observed i.r. and Raman bands in the different phases are listed in Table 1 and the assigned fundamentals belonging to the equatorial and axial conformers are listed in Table 2.

Low temperature solid

The unannealed sample of ECH obtained by shock freezing the vapour on a CsI window (i.r.) or copper block (Raman) at 90 K had an *e*/*a* ratio which was much higher than for the liquid, since the sample was

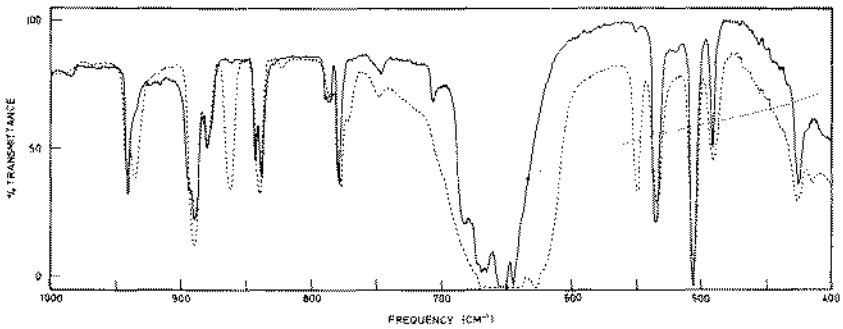

Fig. 1. The i.r. spectra (1000–400 cm^{-1}) of ethynylcyclohexane (ECH) as an amorphous (dotted) and annealed crystalline deposit (solid) at 90 K.

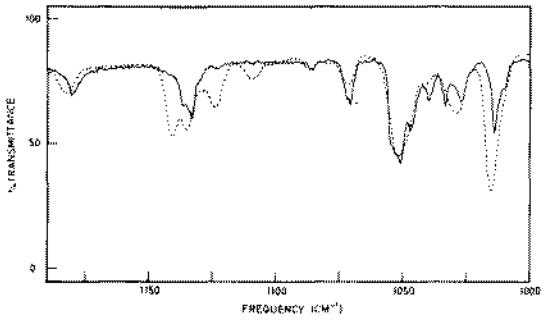

Fig. 2. The i.r. spectra (1185–1000 cm^{-1}) of ECH as an amorphous (dotted) and annealed crystalline deposit (solid) at 90 K.

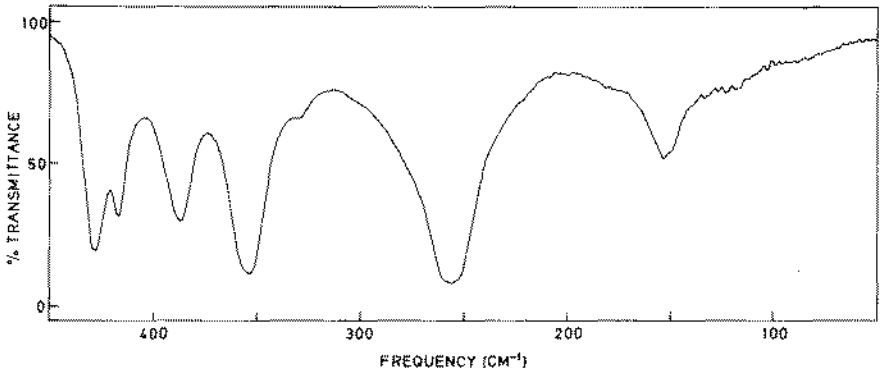

Fig. 3. The far i.r. spectrum (450–60 cm^{-1}) of ECH dissolved in benzene.

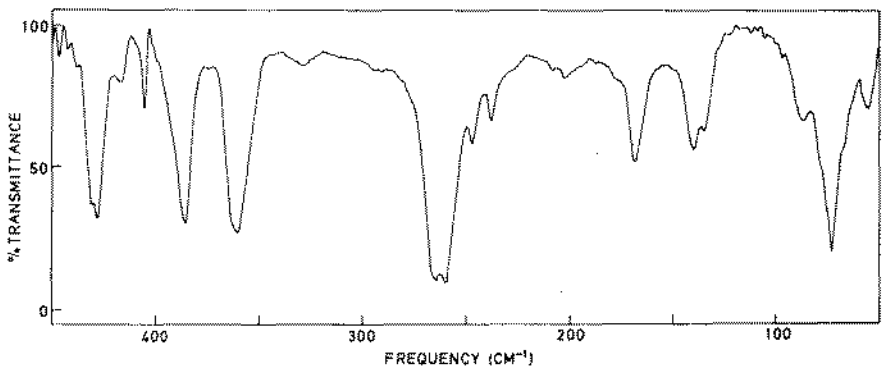

Fig. 4. The far i.r. spectrum (450–60 cm^{-1}) of ECH as an annealed crystalline solid at 90 K.

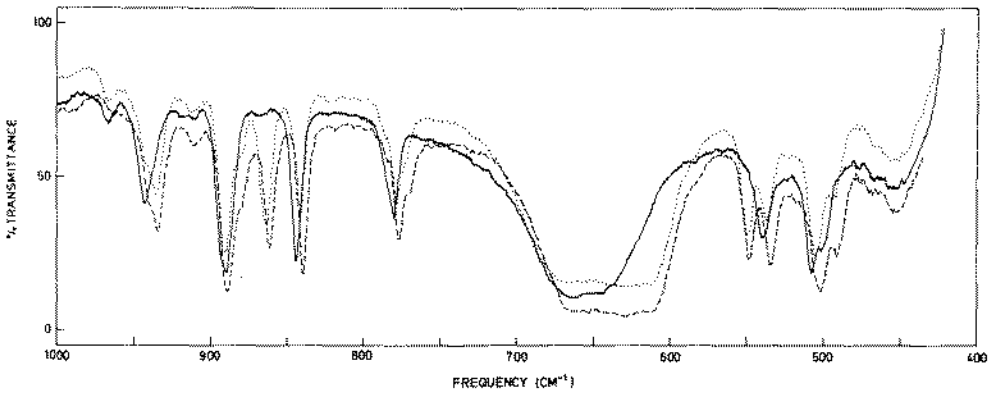

Fig. 5. The i.r. spectra of ECH in the diamond anvil cell; liquid, negligible pressure (dotted curve); liquid, ca 20 kbar pressure (dashed curve); crystalline solid, ca 25 kbar pressure (solid curve).

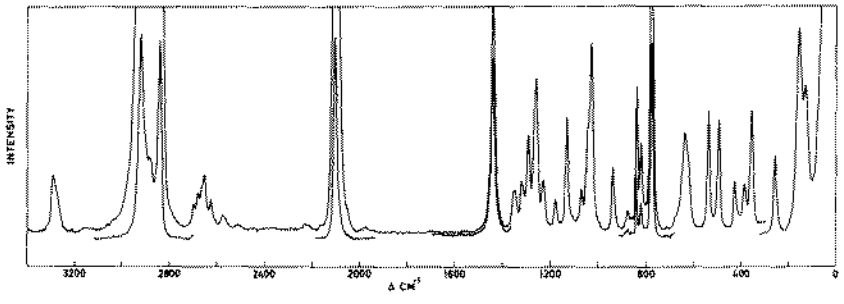

Fig. 6. The Raman spectrum of ECH as a liquid.

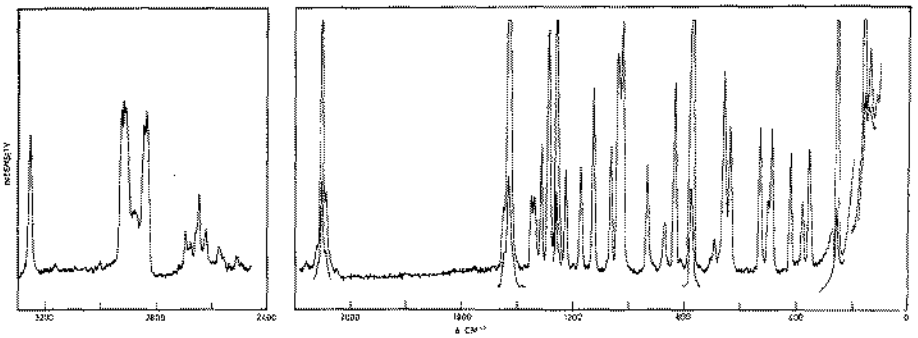

Fig. 7. The Raman spectra of ECH as an annealed crystalline deposit at 90 K.

already partly crystalline. In cyano- and isocyanocyclohexane, on the other hand, the unannealed sample was truly amorphous and maintained the *e*/*a* ratio of the vapour at 300 K [4]. When ECH was annealed to ca 170 K and recooled to 90 K the axial bands had vanished and the equatorial bands frequently showed correlation splitting (e.g. 843/838 cm^{-1}). Clearly, the crystal of ECH contained molecules in the *e*-conformer, unlike cyanocyclohexane [4], but in agreement with other monosubstituted cyclohexanes. While cyanocyclohexane formed a crystalline compound with great difficulty and isocyanocyclohexane in our experiments did not crystallize at all upon cooling [4], ECH formed an anisotropic crystal readily.

High pressure solid

When compressed in the diamond anvil cell, most of the bands shifted towards higher wave numbers and the *a*-bands increased, the *e*-bands decreased in intensity. This effect is clearly seen in Fig. 5 in which the curve recorded at negligible pressure (dashed) has different relative intensities than the one recorded at 20 kbar pressure (dotted-dashed), although in the latter curve all the bands were weaker because of

Table 1. Infrared and Raman spectral data† for ethynylcyclohexane (ECH)

Infrared				Raman		Interpretation	
Liquid	Amorphous solid 90 K	Crystalline solid 90 K	Crystalline solid 25 kbar	Liquid	Crystalline solid 90 K	Equatorial (*e*)	Axial (*a*)
3310 s‡	3305 s	*		3311 m, P	*		$\nu_1 a'$
		3285 w, sh				comb.	
		3279 s					
3292 s, sh	3280 s	3275 vs	3280 vs	3297 m, sh, P	3279 m	$\nu_1 a'$	
		3270 s					
		3260 w, sh				comb.	
		2953 m			2952 m, sh	comb.	
		2943 s		2941 s, P	2945 s	$\nu_2 a'$	$\nu_2 a'$
2932 vs	~2930 vs	2931 s		~2935 s, D?	2936 s	$\nu_3, \nu_{32} a', a''$	$\nu_3, \nu_{32} a', a''$
		2925 s		2923 m, sh, P	2930 s	$\nu_4 a'$	$\nu_4 a'$
2903 s	2900 s	2900 s		2905 m	2898 m	$\nu_5, \nu_{33} a', a''$	$\nu_5 a'$
~2895 m, sh				2899 m			$\nu_{33} a''$
~2870 m, sh		2868 w, sh		~2870 m, sh	2863 s	$\nu_6 a'$	
		2860 m					
		2852 s			2854 m, sh	$\nu_7, \nu_8 a'$	$\nu_6, \nu_7, \nu_8 a'$
2854 s	2852 s	2844 m		2856 s, P	2851 s	$\nu_{34}, \nu_{35} a''$	$\nu_{34}, \nu_{35} a''$
2235 w	2240 vw	2235 vw		2243 vw, P		comb.	comb.
2183 w	2183 vw	*		2175 vw, P?			comb.
	2137 vw			2135 w, sh, P	2141 w	comb.	comb.
2117 m	2118 m, bd	2117 m		2119 s, P	2117 s	$\nu_9 a'$	
2111 m				2115 s, P			$\nu_9 a'$
2097 w, sh	2099 vw	2099 w		2100 w, sh	2101 w	comb.	
				2088 w, sh, P		comb.	
				2067 w, P	2064 w	comb.	
		1463 w					
1462 s	1463 s	1461 m	1462 s	1465 w, P?	1463 m	$\nu_{10} a'$	$\nu_{10} a'$
		1458 w					
		1456 w					
1449 s	1450 s, bd	1453 m	1452 s		1452 w, sh	$\nu_{11}, \nu_{36} a', a''$	$\nu_{36} a''$
		1450 m					
		1446 s	1442 s				
~1445 s, sh	~1445 s, sh	1443 m	1433 s	1445 s	1442 s	$\nu_{12}, \nu_{37} a', a''$	$\nu_{11}, \nu_{37} a', a''$
		1441 m					
		1415 vw				comb.	
		1374 w	*			$\nu_{13} a'$	
		1371 w					
		1362 w					
1361 m	1362 m	1357 m		1361 m, P	1361 m	$\nu_{38} a''$	$\nu_{13}, \nu_{38} a', a''$
		1352 w					
1350 m	1350 m	1347 w	1353 s	1350 m, D	1350 m	$\nu_{39} a''$	$\nu_{14}, \nu_{39}, \nu_{40} a', a''$
1340 w	1344 w, sh	1342 w	1344 w			$\nu_{14} a'$	comb.
	1337 w	1335 w	1337 w			$\nu_{40} a''$	comb.
	1322 w, sh	1322 w	1320 w	1322 m, D	1322 m	$\nu_{15} a'$	$\nu_{41} a''$
		1312 w					
1314 m	1315 m	1306 w		1315 w, P?	*	comb.	$\nu_{15} a'$
		1301 w					
1296 m	1297 m	1299 m	1293 s, bd	1297 s, D	1296 s	$\nu_{41} a''$	
		1296 w					
		1293 m					
1287 w	1287 w	1291 w				comb.	comb.
		1285 w					
	1280 vw	1283 m	1285 w, sh			comb.	
1271 w?	1271 w	1273 vw		1270 s, sh, D	1268 s	$\nu_{16} a'$	$\nu_{42} a''$
		1265 w					
1263 w	1264 w	1263 vw	1266 w	1264 s, P?	*	comb.	$\nu_{16} a'$
		1261 vw					
		1259 vw					
1256 m	1257 m	1256 w	1258 w		1257 m, sh	$\nu_{42} a''$	$2 \times \nu_{25} A'$
		1253 vw					
1234 s	1235 m	1239 w	1232 m	1235 m, P?	1236 m	$\nu_{17} a'$	
		1234 m					
	1229 m, sh	*		1230 m, P	*		$\nu_{17} a'$
		1181 w					
1182 vw	1182 w	1178 w	1184 w	1183 m, D	1182 m	$\nu_{43} a''$	
1140 m	1141 m	*					$\nu_{43} a''$

Table 1. (Continued)

Infrared				Raman		Interpretation	
Liquid	Amorphous solid 90 K	Crystalline solid 90 K	Crystalline solid 25 kbar	Liquid	Crystalline solid 90 K	Equatorial (*e*)	Axial (*a*)
1134 w	1135 m	1137 w 1133 m	1134 w	1134 s, P	1135 s	$\nu_{18}\,a'$	
1123 w	1124 m	*					$\nu_{44}\,a''$
	1110 w	*		1110 vw			$\nu_{18}\,a'$
1100 vw	1101 vw, sh	*	1103 vw, bd?				comb.
	1087 w	1085 vw	1089 vw		1088 vw?	$\nu_{44}\,a''$	
		1074 vw 1073 vw				$\nu_{21}+\nu_{31}\,A'$	
1071 w	1072 w	1071 w 1069 w	1070 w	1073 m, D?	1073 m	$\nu_{45}\,a''$	$\nu_{45}\,a''$
1051 m	1052 m	1054 m 1051 m 1048 w	1053 s	1046 s, P?	1048 s	$\nu_{46}\,a''$	
1040 vw, sh	1040 w	1040 w			1042 m, sh	$\nu_{19}\,a'$	
1029 w	1029 w	1033 w 1027 w	1034 m	1031 s, D	1030 s	$\nu_{20}\,a'$	$\nu_{19}, \nu_{46}\,a', a''$
1013 m	1015 s	1014 m 1011 w	1015 m				$\nu_{20}\,a'$
		1000 vw	997 vw			comb.	comb.
988 vw						comb.	
967 vw	967 vw	*	967 w				$2\times\nu_{27}\,A'$
940 m	941 m	941 m 935 w	943 m	940 m, P	940 m	$\nu_{21}\,a'$	
935 m	935 m		938 w, sh?	932 w, sh			$\nu_{21}\,a'$
	918 vw	924 vw 916 vw	918 vw			$\nu_{47}\,a''$	
910 vw	907 vw		910 vw				$\nu_{47}\,a''$
		906 vw 895 m				$\nu_{25}+\nu_{30}\,A'$, FR	
890 s	890 s	891 s 889 s 887 w	890 s		890 vw, sh	$\nu_{48}\,a''$	
879 w, sh	880 m	882 w 880 m 876 vw	*	880 w, P	879 m	$\nu_{22}\,a'$	
862 m	862 s	862 vw	867 vw	863 w, P?	*		$\nu_{22}, \nu_{48}\,a', a''$
		845 w, sh 843 w 840 w, sh				comb.	
839 s	840 s	839 m 837 w 835 vw	844 s	840 s, P	841 s		$\nu_{23}\,a'$
820 vw	822 w	*	*	822 s, P	820 w		$\nu_{23}\,a'$
784 w, sh	786 w	791 w 786 w	787 w, sh	785 w, D	788 w	$\nu_{49}\,a''$	
777 m	778 s	783 w 779 m 775 vw	780 m	777 s, P	778 s	$\nu_{24}\,a'$	$\nu_{49}\,a''$
771 w	772 m	*	*	772 s, P			$\nu_{24}\,a'$
752 vw							$\nu_{31}+\nu_{50}\,A''$
				712 vw	715 vw?	$2\times\nu_{29}\,A'$	$2\times\nu_{29}\,A'$
704 w, sh					700 w		
		688 s 680 w				$\nu_{52}+\nu_{53}\,A'$, FR	
	672 s, sh	672 s 671 m 669 s			688 m	$\nu_{26}+\nu_{31}\,A'$, FR	
655 m, sh	655 s, bd	656 s 652 m 650 w	~656 vs	639 s, P	664 s	$\nu_{25}\,a'$	$\nu_{25}\,a'$ $\nu_{26}\,a'$
639 s, sh	640 s	646 s 643 w 639 w			644 s	$\nu_{50}\,a''$	
627 vs	627 s	637 w 633 w		629 s, D		$\nu_{27}+\nu_{31}\,A'$	$\nu_{50}\,a''$

Table 1. (Continued)

Infrared				Raman		Interpretation	
Liquid	Amorphous solid 90 K	Crystalline solid 90 K	Crystalline solid 25 kbar	Liquid	Crystalline solid 90 K	Equatorial (*e*)	Axial (*a*)
549 m	551 s	552 vw	*	550 w, D?	*		$\nu_{51}\,a''$
		536 s					
535 m	534 m	534 w, sh	545 s	535 s, P	535 m	$\nu_{26}\,a'$	
		529 w, sh					
503 s	507 s	508 s	512 s	502 m, sh, D?	506 m	$\nu_{51}\,a''$	
492 m	492 m	492 m	502 m	493 s, P	493 m	$\nu_{27}\,a'$	$\nu_{27}\,a'$
456 vw							
		434 w					
427 m	428 m	428 m	431 s	427 s, D	425 m	$\nu_{52}\,a''$	
		425 w, sh					
417 w	416 w	*	*	414 w, sh	*		$\nu_{52}\,a''$
391 w, sh?	391 vw						$\nu_{28}\,a'$
		390 m					
387 m	386 m	385 m	385 m	384 m, P?	383 m	$\nu_{28}\,a'$	
356 m	356 m	363 m	366 m	354 s, P	358 m	$\nu_{29}\,a'$	$\nu_{29}\,a'$
330 vw							
303 vw							
		267 s					
270 w, sh		264 w, sh				$\nu_{30}\,a'$	
256 s	259 s, bd	259 m	260 s	255 s, D	257 m	$\nu_{53}\,a''$	$\nu_{30}\,a'$
252 w, sh§			254 w, sh?				$\nu_{53}\,a''$
		247 w					
		238 w				comb. with lattice modes	
		~200 vw					
154 m§		168 m	163 w	155 s, D	159 s	$\nu_{54}\,a''$	$\nu_{54}\,a''$
140 w, sh?§		140 m	152 w	~140 m, sh	137 m	$\nu_{31}\,a'$	
126 w, sh§		135 w, sh		126 m, D?	*		$\nu_{31}\,a'$
		88 w					
		73 m				lattice modes	
		54 w					

*Asterisks denote bands disappearing in the crystalline state.

†Weak bands in the ranges 5000–3300, 3200–3000, 2800–2300 and 2000–1500 cm^{-1} are omitted because they are outside the regions of fundamentals.

‡Abbreviations: s, strong; m, medium; w, weak; v, very; sh, shoulder; bd, broad; P, polarized; D, depolarized; FR, Fermi resonance.

§Benzene solution.

smaller sample thickness. It is seen that the *a*-bands at 864 and 549 cm^{-1} are enhanced under pressure compared with the *e*-bands at 842 and 837 cm^{-1}. This effect was in qualitative agreement with our results for chloro- and *trans*-1,4-dihalocyclohexanes, in which the axial conformer was ca 1.9–3.8 cm^3/mol smaller in partial molar volume than the equatorial conformer [8]. In all the monohalo-, *trans*-1,2-dihalo- and *trans*-1,4-dihalocyclohexanes we have studied the axial conformer appears to have the smaller volume [9, 10].

When the pressure was increased to ca 25 kbar, ECH crystallized spontaneously to an anisotropic crystal. The solid curve of Fig. 5 reveals that the *a*-bands have vanished and the crystal contains the equatorial conformer like the low temperature crystal.

Thiourea clathrate

By the procedure described previously [11] ECH thiourea clathrates were prepared. The i.r. guest bands were carefully studied in the regions 1000–800 and 600–500 cm^{-1} in which the host bands are weak or of intermediate intensity. In the Nujol mull we observed guest bands at 932 (*a*, *e*), 889 (*e*), 862 (*a*, *e*), 839 (*e*), 548 (*a*), 535 (*e*) and 503 cm^{-1} (*e*). The band intensities of the *e*-bands relative to the *a*-bands in the clathrate and in the liquid suggested an *e*/*a* ratio approximately eight times lower in the clathrate than in the liquid. Thus, the *a*-conformer of ECH is preferred in the thiourea clathrate channels with nearly the same factor as cyano- [11] and isocyanocyclohexane [4].

However, unlike the other types of mono- and disubstituted cyclohexane clathrates we have studied previously [4–6, 11], the ECH thiourea system was not stable with time at the temperature of the P.-E. model 225 i.r. beam (ca 330 K). When the Nujol mull was scanned every ½ h all the guest and host bands changed. The guest band intensities changed, suggesting an increased *e*/*a* ratio. Independently, the rhombohedral thiourea bands at 654 and 615 cm^{-1} diminished, whereas the orthorhombic bands at 630, 488 and 460 cm^{-1} increased in intensities (see Table 1, Ref. [11]). These changes strongly suggest that the

Table 2. Observed* and calculated fundamental frequencies for ethynylcyclohexane

	Equatorial (*e*)			Axial (*a*)		
	PED†	Obs.	Calc.	PED	Obs.	Calc.
a'						
ν_1	$95d(l)$‡	3292	3301	$95d(l)$	3310	3301
ν_2	$97d(X)$	2941	2958	$98d(X)$	2941	2958
ν_3	$94d$	2932	2922	$96d$	2932	2922
ν_4	$95d$	2923	2916	$95d$	2923	2916
ν_5	$96d$	2903	2914	$98d$	2903	2914
ν_6	$95d$	2860	2857	$96d$	2854	2857
ν_7	$97d$	2854	2853	$95d$	2854	2854
ν_8	$96d$	2854	2851	$95d$	2854	2851
ν_9	$84l+11X$	2119	2117	$84l+11X$	2115	2117
ν_{10}	$73\delta+20\gamma$	1462	1456	$73\delta+17\gamma$	1462	1456
ν_{11}	$65\delta+20\gamma$	1449	1439	$64\delta+21\gamma$	1445	1437
ν_{12}	$60\delta+19\gamma+10R$	1440	1426	$67\delta+27\gamma$	1425§	1422
ν_{13}	$36\gamma+20\theta+15R$	1372	1386	$33\gamma+28\theta+14\gamma\ (X)$	1361	1360
ν_{14}	$76\gamma+15R$	1345	1343	$73\gamma+14R$	1350	1346
ν_{15}	$40\gamma+33\theta+14\gamma\ (X)$	1322	1295	$45\gamma+20\theta+12R$	1314	1333
ν_{16}	$73\gamma+12R$	1270	1253	$70\gamma+15R$	1263	1263
ν_{17}	74γ	1234	1231	77γ	1229	1230
ν_{18}	$62\gamma+10R$	1134	1134	$51\gamma+10X$	1110	1135
ν_{19}	$37X+20\omega+17\gamma$	1040	1043	$49R+34\gamma$	1029	1031
ν_{20}	$40R+34\gamma$	1030	1023	$39\gamma+39\omega$	1013	1006
ν_{21}	$34\gamma+26X+20R$	940	927	$32\gamma+26X+23R$	935	934
ν_{22}	$44\gamma+29R$	880	893	$50\gamma+30R$	862	858
ν_{23}	$58R+25\gamma$	840	834	$55R+20\gamma$	822	815
ν_{24}	$38R+29\gamma$	777	767	$36R+19X+17\gamma$	771	783
ν_{25}	97β	639	635	$20X+17\gamma+13\omega+12R+10\beta$	655	646
ν_{26}	$31\gamma+24\omega$	535	535	84β	639	632
ν_{27}	$22\gamma+20\omega+20\alpha+10\gamma\ (X)$	492	501	$40\omega+35\gamma$	492	493
ν_{28}	59ω	387	403	$51\omega+16\Xi+12\tau$	391	393
ν_{29}	$36\omega+33\tau+13\alpha$	356	361	$45\alpha+21\omega+18\tau$	356	354
ν_{30}	$38\alpha+23\tau+18\omega$	270	277	$29\tau+24\alpha+24\omega+10\Xi$	255	274
ν_{31}	$29\tau+26\alpha+14\Xi+13\omega$	137	132	$28\tau+23\alpha+13\Xi+13\omega$	126	108
a''						
ν_{32}	$98d$	2932	2917	$97d$	2932	2918
ν_{33}	$97d$	2903	2913	$97d$	2899	2913
ν_{34}	$97d$	2854	2855	$97d$	2854	2855
ν_{35}	$97d$	2854	2852	$97d$	2854	2852
ν_{36}	$72\delta+16\gamma$	1449	1442	$77\delta+17\gamma$	1449	1440
ν_{37}	$62\delta+19\gamma$	1445	1432	$58\delta+19\gamma+10R$	1445	1433
ν_{38}	$52\gamma+24R+16\gamma\ (X)$	1361	1378	$67\gamma+21R$	1361	1368
ν_{39}	$73\gamma+10R$	1350	1347	86γ	1350	1350
ν_{40}	$73\gamma+10R$	1337	1345	69γ	1350	1340
ν_{41}	$69\gamma+16\gamma\ (X)$	1296	1301	$29R+28\gamma\ (X)+28\gamma$	1322	1300
ν_{42}	$73\gamma+15\gamma\ (X)$	1256	1244	75γ	1271	1255
ν_{43}	$66\gamma+19R$	1183	1189	$64\gamma+16R$	1140	1158
ν_{44}	$49R+36\gamma$	1087	1097	$67\gamma+16R$	1123	1137
ν_{45}	$67\gamma+18\gamma\ (X)$	1073	1071	$58\gamma+30R$	1071	1079
ν_{46}	$65R+25\gamma$	1051	1053	$59R+23\gamma$	1029	1035
ν_{47}	$44\gamma+28R$	918	912	80γ	910	934
ν_{48}	$51\gamma+31R$	890	890	$67R+15\gamma$	862	857
ν_{49}	$72\gamma+14R$	784	789	$71\gamma+14R$	777	789
ν_{50}	97β	639	635	97β	629	634
ν_{51}	$41\Xi+41\alpha$	503	488	$42\Xi+25\alpha+14\omega$	549	544
ν_{52}	64ω	427	459	$49\omega+13\alpha$	417	434
ν_{53}	$45\omega+42\tau$	255	227	$36\alpha+24\tau+22\omega$	252	251
ν_{54}	$57\alpha+31\Xi$	155	164	$35\alpha+27\Xi+16\omega+10\tau$	155	145

*When possible frequency values taken from the liquid spectra are given.

†The potential energy distribution defined as $100\,F_{ii}\,L_{ik}^2 / \sum_i F_{ii}\,L_{ik}^2$.

‡$d(X)$ and $\gamma(X)$, C–H stretching and CCH bending in the X–C–H (X, HC≡C) group; d and γ, CH stretchings and CCH bendings in the C–CH_2 groups; R, C–C stretchings in the ring; X, C–C stretching in the HC≡C–C group; δ, H–C–H bendings; θ, H–C–X (X, HC≡C) bending; Ξ, C–C–X (X, HC≡C) bending; l, C≡C stretching; $l(d)$, C–H stretching in the H–C≡C group; α, C–C≡C bending, β, C≡C–H bending; τ, torsions around the C–C bonds in the ring (see Ref. [13]).

§Observed only in the Raman spectrum of the amorphous solid.

ECH thiourea clathrate is unstable at ca 330 K and disintegrates into the free thiourea (orthorhombic) and liquid ECH with time. No disintegration was detected at ambient temperature and the clathrate could be stored for days with no apparent changes. We have no ready explanation why the ECH thiourea clathrate should be more unstable than the 11 cyclohexane thiourea clathrates studied previously.

Spectral interpretation

The enhancement of the axial bands of ECH upon compressing and in the thiourea clathrate confirms our conclusion that the equatorial conformer is present in the anisotropic crystal. Independent support is provided by the results of the normal coordinate analysis and the spectral correlations with cyano- and isocyanocyclohexane. The "spectral indicator" (the band between 585 and 650 cm^{-1}), supposedly characteristic for axially substituted cyclohexanes [12], cannot be applied to ECH since the very intense C≡C–H bending modes (one a' and one a'' for each conformer) cover this region.

With 20 atoms in the molecule and C_s symmetry, ECH should have 31 fundamentals of species a' and 23 a'' for each conformer. As a first approximation we expect one acetylenic C–H stretch of species a' around 3300 cm^{-1} and two acetylenic C–H bending modes of species a' and a'' around 640 cm^{-1} for each conformer in addition to the bands observed for cyano- and isocyanocyclohexanes [4]. Moreover, the cyano (C≡N) and isocyano (N≡C) stretching modes at 2240 and 2140 cm^{-1}, respectively [4] will in ECH be interchanged with the acetylenic (C≡C) stretch at 2119 cm^{-1}.

The assignments were based upon the usual criteria described in the previous paper [4] and the results are listed in Table 2. Obviously, the results of the normal coordinate analysis were of particular help in the interpretation, especially for deciding the cases of coinciding equatorial and axial conformers. As is apparent from Table 2, the agreement between the observed and calculated wave numbers is quite good for ECH as well as for cyano- and isocyano- [4] and *trans*-1,4-dicyanocyclohexane [7] which were treated together in the calculations (see below).

Force constant calculations. Force fields for the ethynyl-, cyano- and isocyanocyclohexanes were derived by transferring force constants for the monohalo- and *trans*-1,4-dihalocyclohexanes [13] and for propyne, methylcyanide and methylisocyanide [14]. Only the diagonal, one stretch/stretch and four stretch/bend interaction force constants involving the coordinates of the substituents and of the substituted sites in the cyclohexane ring were refined in

Table 3. Valence force constants for ethynyl- (E), cyano- (C) and isocyanocyclohexane (I)

Force constant	Group	Coordinate(s) involved	Atoms common to interacting coordinates	Calculated value θ_i	Standard error $\sigma(\theta_i)$
Stretch[a]				(mdyn·Å)[b]	
K_d	C–CH_2–C	C–H	—	(5.413)[c]	
$K_d(X)$[d]	C–CHX–C	C–H	—	(5.683)	
$K_d(I)$	C≡C–H	C–H	—	6.534	0.035
K_R	(C)–C–C–(C)	C–C	—	(10.36)	
$K_R(X)$	(C)–C–C–(X)	C–C	—	10.87	0.26
$K_X(E)$	C–C≡C	C–C	—	11.44	0.59
$K_X(C)$	C–C≡N	C–C	—	10.65	0.37
$K_X(I)$	C–N≡C	C–N	—	10.56	0.49
$K_t(E)$	C≡C	C≡C	—	22.60	0.27
$K_t(C)$	C≡N	C≡N	—	23.75	0.15
$K_t(I)$	N≡C	N≡C	—	22.35	0.22
Bend				(mdyn Å rad^{-2})	
H_δ	C–CH_2–C	HCH	—	(0.5055)	
H_γ[e]	C–CH_2–C	HCC	—	(0.6450)	
$H_\theta(E)$	H–C–C≡	HCC	—	0.759	0.029
$H_\theta(C)$	H–C–C≡	HCC	—	0.785	0.021
$H_\theta(I)$	H–C–N≡	HCN	—	0.821	0.027
H_ω	C–CH_2–C	CCC	—	(0.913)	
$H_\omega(X)$	C–CHX–C	CCC	—	1.166	0.059
$H_\Xi(E)$	C–C–C≡C	CCC	—	1.06	0.10
$H_\Xi(C)$	C–C–C≡N	CCC	—	0.939	0.059
$H_\Xi(I)$	C–C–N≡C	CCN	—	0.975	0.083
$H_\alpha(E)$	C–C≡C	CCC	—	0.365	0.033
$H_\alpha(C)$	C–C≡N	CCN	—	0.310	0.018
$H_\alpha(I)$	C–N≡C	CNC	—	0.176	0.021
H_β	C≡C–H	CCH	—	0.2282	0.0040
Torsion[f]				(mdyn Å rad^{-2})	
τ	CHX–C^*H_2–C‡H_2	C†–C‡	—	(0.0161)	
$\tau(X)_a$	CHX–CH_2	C–C	—	0.072	0.011
$\tau(X)_b$	CHX–CH_2	C–C	—	0.0708	0.0083
τ_s	CH_2–CH_2	C–C	—	(0.0437)	

Table 3. (Continued)

Force constant	Group	Coordinate(s) involved	Atoms common to interacting coordinates	Calculated value θ_i	Standard error $\sigma(\theta_i)$
Stretch–stretch				(mdyn Å)[b]	
F_d	C–CH_2–C	C–H, C–H	C	(0.023)	
F_R	C–C–C	C–C, C–C	C	(0.701)	
F_{RX}	C–C–X	C–C, C–X	C	0.78	0.15
F_{Xl}	C–C≡Y[g]	C–C, C≡Y	C	(0.5)	
Stretch–bend				(mdyn Å rad^{-1})[b]	
$F_{R\gamma}$	C–CH_2–C	C–C, HCC	C–C	(0.106)	
$F_{X\theta}$	C–CHX–C	C–X, HCX	C–X	1.00	0.11
$F'_{R\gamma}$	C–CH_2–C	C–C, HCC	C	(−0.268)	
$F_{R\omega}$	C–C–C	C–C, CCC	C–C	(0.393)	
$F_{R\equiv}$	C–C–X	C–C, CCX	C–C	0.33	0.12
$F_{X\equiv}$	C–C–X	C–X, CCX	C–X	0.931	0.094
$F_{X\omega}$	C–CHX–C	C–X, CCC	C	−0.15	0.12
Bend–bend				(mdyn Å rad^{-2})	
F_γ	C–CH_2–C	HCC, HCC	C–C	(−0.0227)	
F'_γ	C–CH_2–C	HCC, HCC	H–C	(0.0041)	
$F_{\gamma\theta}$[h]	C–CHX–C	HCC, HCX	H–C	(0.0041)	
$F_{\gamma\omega}$[h]	C–CH_2–C	HCC, CCC	C–C	(−0.090)	
f^t_γ	–CH_2–CH_2–	H_aCC, H_b CC	$(H_a)C^{trans}C(H_b)$	(0.0735)	
f^g_γ	–CH_2–CH_2–	H_aCC, H_bCC	$(H_a)C^{gauche}C(H_b)$	(−0.0687)	
$f^{t'}_\gamma$	–CH_2–C^+H_2–C‡–	H_aCC^+, H_bCC‡	$(C–CH_b)–C^+(H_a)$	(−0.0337)	
$f^{g'}_\gamma$	–CH_2–C^+H_2–C‡–	H_aCC^+, H_bCC‡	$(C–CH_b)–C^+(H_a)$	(−0.0293)	
f^{tt}_γ	C^+CH_2–CH_2–C‡	H_aCC^+, H_bCC‡	$(C–CH_a)–(CH_b–C)$	(−0.0187)	
$f^{gg'}_\gamma$	C^+CH_2–CH_2–C‡	H_aCC^+, H_bCC‡	$(C–CH_a)–(CH_b–C)$	(−0.0309)	
$f^t_{\gamma\omega}$[i]	C–C–CH_2	HCC, CCC	$(H)–C^{trans}C–(C)$	(0.0759)	
$f^g_{\gamma\omega}$[j]	C–C–CH_2	HCC, CCC	$(H)–C^{gauche}C–(C)$	(−0.0307)	
f^g_{ω}[k]	C–C–C–C	CCC, CCC	$(C)–C^{gauche}C–(C)$	(−0.024)	
F	C–C≡C–H	CCC, CCH	C≡C	(0.129)	

[a] Internal coordinates and symbols are defined in Refs. [13, 15, 16].
[b] The stretch, stretch–stretch and stretch–bend constants in the conventional units are listed in Table 4.
[c] If a force constant is in parentheses, its value was not adjusted in the refinement.
[d] X=C≡C–H, C≡N or N≡C.
[e] $H_\gamma = H_\tau(X)$.
[f] The torsion is defined as a normalized sum of three *trans* torsions.
[g] Y = C or N.
[h] $F_{\gamma\omega} = F_{\theta\equiv}$.
[i] $f^t_{\gamma\omega} = f^t_{\theta\omega}$.
[j] $f^g_{\gamma\omega} = f^g_{\theta\omega}$.
[k] $f^g_\omega = f_{\omega\neq}$.

Table 4. The stretch, stretch–stretch and stretch–bend force constants in conventional units

Stretch* (mdyn $Å^{-1}$)		Stretch–stretch (mdyn $Å^{-1}$)		Stretch–bend (mdyn rad^{-1})			
K_d	4.531	F_d	0.019	$F_{R\gamma}$	0.069	$F_{X\omega}(E)$	−0.101
$K_d(X)$	4.757	F_R	0.296	$F_{X\theta}(E)$	0.671	$F_{X\omega}(C)$	−0.101
$K_d(l)$	5.815	$F_{RX}(E)$	0.340	$F_{X\theta}(C)$	0.676	$F_{X\omega}(I)$	−0.103
K_R	4.368	$F_{RX}(C)$	0.342	$F_{X\theta}(I)$	0.690		
$K_R(X)$	4.583	$F_{RX}(I)$	0.349	$F_{R\gamma}$	−0.174		
$K_X(E)$	5.153	$F_{Xl}(E)$	0.278	$F_{R\omega}$	0.255		
$K_X(C)$	4.862	$F_{Xl}(C)$	0.294	$F_{R\equiv}$	0.214		
$K_X(I)$	5.022	$F_{Xl}(I)$	0.300	$F_{X\equiv}(E)$	0.625		
$K_l(E)$	15.513			$F_{X\equiv}(C)$	0.629		
$K_l(C)$	18.021			$F_{X\equiv}(I)$	0.642		
$K_l(I)$	16.959						

*For definition of symbols, see Table 3.

the present calculation. The rest of the force constants were constrained to their transferred values. The structural parameters were taken as follows: C–C = 154.0 pm, C–H = 109.3 pm, C–H = 106.0 pm, (C≡)C–C = 149.0 pm, (N≡)C–C = 148.0 pm, (C≡)N–C = 145.0 pm, C≡C = 120.7 pm, –C≡N = 114.8 pm, –N≡C = 114.8 pm and all of the valence angles tetrahedral, except in the linear side chains.

We have used dimensionless internal stretching coordinates, i.e. $\Delta r/r_e$, and thereby have been able to reduce by approximation the number of different parameters in the force field [11]. The final set of force constants, adjusted by the least squares method, are given in Table 3. For the sake of easy comparison with the force constants of other authors the stretch, stretch–stretch and stretch–bend interaction constants are given in terms of the usual units in Table 4.

REFERENCES

[1] H.-J. SCHNEIDER and V. J. HOPPER, *J. org. Chem.* **43**, 3866 (1978).
[2] F. R. JENSEN, C. H. BUSHWELLER and B. H. BECK, *J. Am. chem. Soc.* **91**, 344 (1969).
[3] G. DIAMINI, G. CORBELLI and F. SCAPPINI, *J. molec. Struct.* **63**, 221 (1980).
[4] T. WOLDBAEK, A. BERKESSEL, A. HORN and P. KLAEBOE, *Acta chem. scand.* **A36**, 719 (1982).
[5] S. D. CHRISTIAN, J. GRUNDNES, P. KLAEBOE, E. TØRNENG and T. WOLDBAEK, *Acta chem. scand.* **A34**, 391 (1980).
[6] T. WOLDBAEK, *Acta chem. scand.* **A36**, 641 (1982).
[7] O. H. ELLESTAD, P. KLAEBOE and T. WOLDBAEK, *J. molec. Struct.* **95**, 117 (1982).
[8] S. D. CHRISTIAN, J. GRUNDNES and P. KLAEBOE, *J. Am. chem. Soc.* **97**, 3864 (1975).
[9] P. KLAEBOE, *Z. Chem., Leipzig* **21**, 471 (1982).
[10] C. E. SJØGREN and P. KLAEBOE, *J. molec. Struct.* **100**, 433 (1983).
[11] J. E. GUSTAVSEN, P. KLAEBOE and H. KVILA, *Acta chem. scand.* **A32**, 25 (1978).
[12] G. N. ZHIZHIN and KH. E. STERIN, in *Vibrational Spectra and Structure*, vol. 9, p. 195 (edited by J. R. DURIG). Elsevier, Amsterdam (1981).
[13] T. WOLDBAEK, C. J. NIELSEN and P. KLAEBOE, *J. molec. Struct.* **66**, 31 (1980).
[14] J. L. DUNCAN, *Spectrochim. Acta* **20**, 1197 (1964).
[15] R. G. SNYDER and J. H. SCHACHTSCHNEIDER, *Spectrochim. Acta* **21**, 169 (1965).
[16] R. G. SNYDER and J. H. SCHACHTSCHNEIDER, *J. molec. Spectrosc.* **30**, 290 (1969).